

# Biocalorimetric monitoring of photoautotrophic batch cultures

Marcel Janssen<sup>a,b,\*</sup>, René Wijffels<sup>b</sup>, Urs von Stockar<sup>a</sup>

<sup>a</sup> *Laboratory of Chemical and Biological Engineering, Federal Institute of Technology, Lausanne, Switzerland*

<sup>b</sup> *Food and Bioprocess Engineering Group, Wageningen University and Research Centre, P.O. Box 8129, 6700 EV Wageningen, The Netherlands*

Available online 14 January 2007

## Abstract

Cultivations of photoautotrophic microorganisms show a rather distinct behavior from the cultivations of microorganisms on chemical energy. This is caused by the fact that light energy is the limiting substrate. Light supply is characterized by a constant photon flux which cannot be stored within the culture broth.

In this study batch cultivations of *Chlorella sorokiniana* were closely followed in a bench-scale biocalorimeter (1.63 L, Ø 11.6 cm) illuminated with red light emitting diodes. Calorimetry provided the rate of light energy storage inside biomass representing chemical energy. Normalized to the total input of light energy this yielded the photosynthetic efficiency. It was highest in the beginning of the batch cultures: 14% at a cell density of less than 1 mL cells L<sup>-1</sup>. Efficiency decreased to 5.4% as cell density increased further to 5 mL cells L<sup>-1</sup> (=2.5 g L<sup>-1</sup>). Efficiency was highest at low cell density when light penetrates far inside the reactor. Our results support previous findings that the presence of an increasing dark zone leads to reduced photosynthetic efficiency.

The same trend was detected using measurements of carbon dioxide and ammonium consumption. The carbon dioxide consumption rate was used to calculate the enthalpy increase in the culture broth during photoautotrophic growth. The maximum photosynthetic efficiency calculated from the enthalpy increase was higher than the one measured directly in the biocalorimeter: 16% as opposed to 14%. This discrepancy probably is related to a combination of factors which are discussed opening up possibilities for further improvement of this technique.

© 2007 Elsevier B.V. All rights reserved.

**Keywords:** Biocalorimetry; Microalgae; Photosynthetic efficiency; *Chlorella*; Batch cultivation

## 1. Introduction

Bench-scale calorimetry is a powerful tool for on-line monitoring of microbial processes in bioreactors under controlled conditions [1]. In combination with other on-line analytics such as off-gas analysis and/or liquid analyses for metabolite exchange, insight in metabolism can be greatly improved [2–4]. Phototrophic processes such as the cultivation of microalgae receive warm attention of scientists within the field of biocalorimetry. This did not result yet in significant scientific progress. The lack of progress seems to be related to technical limitations associated with the design of photobioreactors and the need for heat-generating light sources. The work done until now has been carried out in millilitre-scale calorimeters [5–8], and only the work of Magee et al. [5] produced new insights into

photoautotrophic metabolism. In 1939 they determined a quantum yield of 0.077 supporting the Z-scheme of photosynthesis developed in that time [9].

The functioning of photosynthesis is largely understood nowadays. A potential role for photobiocalorimetry therefore should be related to process monitoring and control, and quantifying the magnitude of known effects such as the dissipation of photons at (over)-saturating light intensity. For the same purpose other techniques are available, but combining different measurements will lead to more reliable data and better insight in the metabolic state of the process.

In previous studies we have shown that a bench-scale BioRC1 calorimeter (2 L) can be adapted for the cultivation of phototrophic microalgae [10,11]. Using the green microalga *Chlorella vulgaris* we measured endothermic heat flows under photo-heterotrophic growth conditions as compared to an exothermic heat flow under chemo-heterotrophy [10]. In a follow-up, under strictly photoautotrophic conditions, we demonstrated that the photosynthetic allocation of light energy to chemical energy can be quantified directly measuring the change in the biochemical heat flow in a BioRC1 [11]. In

\* Corresponding author. Present address: Food and Bioprocess Engineering Group, Wageningen University and Research Centre, P.O. Box 8129, 6700 EV Wageningen, The Netherlands. Tel.: +31 317 484708; fax: +31 317 482237.

E-mail address: [marcel.janssen@wur.nl](mailto:marcel.janssen@wur.nl) (M. Janssen).

this study we measured an increase of power generated in the biocalorimeter when illumination was switched on and biomass started growing. In photosynthesis only a part of the light energy can be stored as chemical energy (i.e. biomass). The remainder of the light energy (>75%) is lost as heat by a combination of processes occurring directly after light absorption within the microalgal photosystems, or, is lost further downstream within the biochemical reaction pathways of photoautotrophic metabolism.

In order to quantify the exact amount of light energy stored, the total light input needs to be measured. In our previous work this was done inhibiting phototrophic metabolism using specific inhibitors. The power in the biocalorimeter increased to a maximal level [11]. The difference between this level and biocalorimeter power with actively photosynthesizing biomass gave the amount of light energy stored as chemical energy. This study was referred to as an exothermic process by others [8]. This is true if one takes the biocalorimeter power with illumination turned off as the reference situation. But, if one takes the maximal power level, with non-active biomass and illumination turned on, as the reference situation, photosynthesis leads to an endothermic signal: light-induced heat disappears due to the action of photosynthesis.

Although it was shown to be possible to measure photosynthetic activity this could only be done for one arbitrary moment in time during batch cultivations of *Chlorella*. In the present study we set a step further monitoring photosynthetic light energy consumption during the whole batch cultivation of several days. This was made possible increasing the light input and improving the even distribution of light energy across the bioreactor surface. Furthermore, the influence of fluctuations in ambient temperature on biocalorimeter power was monitored and modeled. This led to an improved signal-to-noise ratio and made it possible to monitor the process for several days.

Photosynthetic conversion of light energy into chemical energy was measured on-line in our adapted BioRC1 calorimeter during photoautotrophic cultures of *Chlorella sorokiniana*. It was observed that the photosynthetic efficiency quickly reached a maximum at low cell density and then slowly decreased as cell density increased further. These results will be discussed with respect to existing knowledge on photoautotrophic cultures. The performance of the calorimetric measurement will be compared with other methods, such as that of the carbon dioxide consumption rate, and the technical shortcomings of photobiocalorimetry, still present, will be discussed.

## 2. Experimental

### 2.1. Organism and medium

*C. sorokiniana* (Chlorophyta) CCAP 211/8K was derived from the Culture Collection of Algae and Protozoa (CCAP, Oban, Scotland). The cultivation medium was based on the one described by Mandalam and Palsson [12] and was composed of (in mmol L<sup>-1</sup>): KNO<sub>3</sub>, 29.7; KH<sub>2</sub>PO<sub>4</sub>, 5.44; Na<sub>2</sub>HPO<sub>4</sub>·2H<sub>2</sub>O, 1.46; MgSO<sub>4</sub>·7H<sub>2</sub>O, 1.62; CaCl<sub>2</sub>·2H<sub>2</sub>O, 0.088. In addition, the following (trace) elements were added (in μmol L<sup>-1</sup>): EDTA

ferric sodium salt, 316; Na<sub>2</sub>EDTA·2H<sub>2</sub>O, 100; H<sub>3</sub>BO<sub>3</sub>, 1.00; MnCl<sub>2</sub>·4H<sub>2</sub>O, 65.6; ZnSO<sub>4</sub>·7H<sub>2</sub>O, 11.1; CuSO<sub>4</sub>·5H<sub>2</sub>O, 7.33. The pH was set to 6.7 with 4N NaOH.

*C. sorokiniana* was maintained under aseptic conditions in 100 mL liquid cultures in 250 mL glass Erlenmeyer flasks closed with cotton stoppers. Every 2 weeks cultures were transferred to new flasks with freshly prepared medium. The flasks were placed under mild fluorescent light ( $\pm 20 \mu\text{mol m}^{-2} \text{s}^{-1}$ ) at room temperature on an orbital shaker (100 rpm). They were illuminated 24 h day<sup>-1</sup>.

### 2.2. Photobiocalorimeter and illumination

A modified 2 L commercial reaction calorimeter, RC1 from Mettler-Toledo AG (Greifensee, Switzerland) was used, the BioRC1. The software and hardware of this calorimeter were modified to increase the resolution as described elsewhere [13,14]. Some of the modifications presented and tested by García-Payo et al. [15] were also applied (Fig. 1): the head plate temperature was maintained at  $T_r + 2^\circ\text{C}$  and the modified version of the standard glass RC1 reactor was used.

As can be seen in Fig. 1 the reactor was surrounded by a polycarbonate cylinder to prevent convective heating of the reactor by warm air coming from the lamps. Light energy was supplied via a light source based on light emitting diodes (LEDs) (Fig. 1). A number of 60 strips each composed of 15 LEDs were placed vertically on a metal frame completely surrounding the bioreactor. The LED type used was a 5 mm AlInGaP, type YZ-R5N30 (Yoldal Co. Ltd., Taiwan), with a wavelength of 625 nm. The radiation emitted by the LED completely falls within the absorption range of chlorophyll-rich green microalgae and is suitable for the cultivation of *Chlorella* [16]. Above all, water, glass and polycarbonate hardly absorb radiation with a wavelength lower than 700 nm. Aluminum foil was attached on the lower and higher part of the polycarbonate cylinder as to make sure that the lamps only illuminated that part of the reactor surface that was filled with culture broth (Fig. 1).

The LED strips were mounted on a perforated metal cylinder and between adjacent strips there was an empty space, all allowing for convection around the LED strips. Four ventilators were positioned behind the light source blowing air on the rear of the LED strips. This was necessary to cool the LEDs, minimizing any decrease in LED output. The light intensity at the reactor surface was continuously measured using a US-SQS spherical micro quantum sensor (Heinz-Walz GmbH, Effeltrich, Germany). The sensor was placed at an arbitrary position against the reactor surface (Fig. 1). The reactor surface behind the sensor was darkened with a small piece (1 cm<sup>2</sup>) of black tape to prevent light coming out of the bioreactor (at low biomass densities) to reach the spherical sensor.

The reactor temperature ( $T_r$ ) was continuously monitored and maintained at  $37^\circ\text{C} \pm 0.5^\circ\text{mC}$  by adapting the oil temperature in the cooling jacket ( $T_j$ ) until a steady-state is reached, i.e. heat-conduction calorimetry. In this situation the temperature gradient between the culture suspension and cooling jacket ( $T_r - T_j$ ) is such that the rate of heat transfer exactly matches the rate of heat generation. This temperature gradient

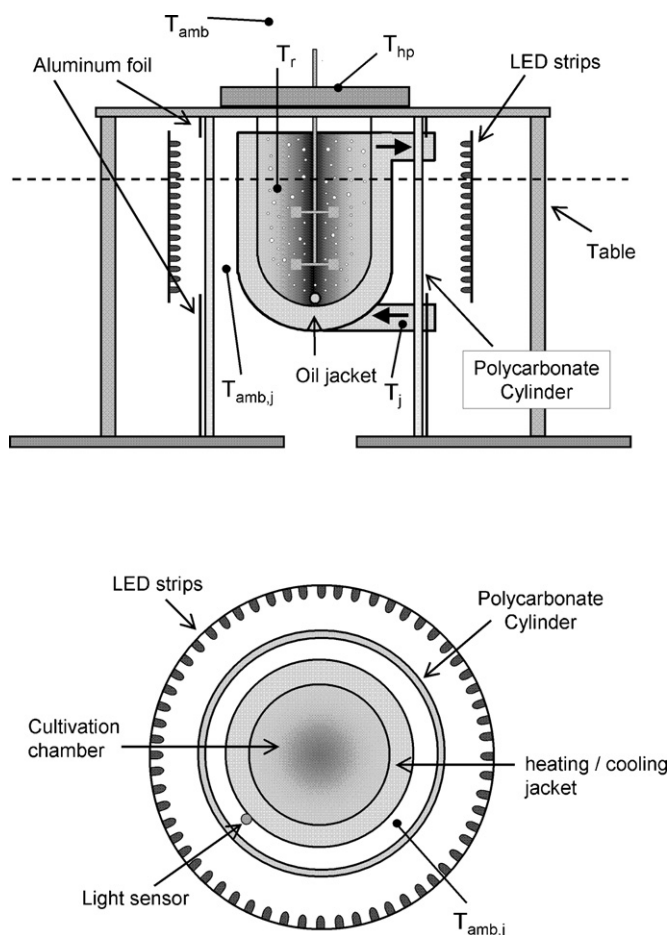


Fig. 1. Schematic presentation of the BioRC1 calorimeter hanging in the table and surrounded by the circular LED-based light source. The culture is continuously gassed with an  $O_2/CO_2/N_2$  mixture and mixed by a mechanical turbine stirrer. The dashed line in the upper drawing represents the height at which the cross section, the lower drawing, is made. The positions of different temperature sensors are also indicated. Abbreviations:  $T_r$ , temperature reactor liquid;  $T_j$ , temperature ingoing oil BioRC1 cooling jacket;  $T_{amb}$ , ambient temperature;  $T_{amb,j}$ , temperature air between reactor jacket and polycarbonate cylinder;  $T_{hp}$ , temperature reactor head plate.

is continuously adapted by the BioRC1 control circuitry as a response to changes in heat production rate. Using a calibration heater, the heat transfer coefficient of the cooling jacket is determined regularly and this coefficient is used to quantify the heat rate (power,  $P$ ) during the actual biological processes (Eq. (1)).

$$P = UA \cdot (T_r - T_j) \quad (1)$$

The culture broth was mixed at 300 rpm using two six-blade disc turbines connected to the central stirrer shaft. The culture was gassed with an oxygen/carbon dioxide/nitrogen mixture (18/2/80%, v/v/v) to provide carbon dioxide and to remove oxygen. The flow was controlled with a mass flow controller (Brooks Instruments BV, The Netherlands) and set at  $200 \text{ mLn min}^{-1}$  (mLn, mL of gas under normal conditions,  $0^\circ\text{C}$  and standard pressure). The gas was humidified and heated prior to entering the biocalorimeter limiting the influence of evaporation and gas temperature fluctuations on the stability of the power baseline.

After passing through a  $0.2 \mu\text{m}$  filter, the gas was dispersed as very fine bubbles at the bottom of a 2 L DURAN bottle (Schott, Germany) filled with 2 L of water maintained at  $50^\circ\text{C}$ . Subsequently, the gas was led through a similar bottle maintained at  $T_r + 2^\circ\text{C}$  before it was released in the reactor.

The reactor was equipped with a pH and a Clark-type dissolved oxygen (DO) probe to monitor both variables continuously. The pH was controlled at 6.7 by automatic addition of ammonium hydroxide solution (160 mM) and the addition rate was measured gravimetrically.

### 2.3. Experimental procedure

Two characteristic batch experiments will be presented and discussed. First, the reactor was filled with de-mineralized water and autoclaved in situ ( $121^\circ\text{C}$ ) with all probes in place. The humidifying bottles, tubing and filters used for the gas supply were autoclaved separately at  $121^\circ\text{C}$  and connected to the BioRC1 after cooling down. The bottle for the ammonium hydroxide solution was autoclaved separately and filled with the alkaline solution afterwards. All other reactor connections, tubing for sampling, medium or base addition, and the gas outlet were autoclaved separately and connected to the BioRC1 just after it cooled down.

After connecting the in- and outlets, the gas flow was started and the water was slowly released via a drain at the bottom of the reactor. The BioRC1 was filled with sterile medium and started in the isothermal ( $T_r$ ) mode at  $37.000^\circ\text{C}$ . The medium was sterilized by filtration over a  $0.22 \mu\text{m}$  filter. It was the same as the medium described for culture maintenance only ammonium was used as the nitrogen source at 2 mM and the pH was not set beforehand; additional ammonium was added continuously via the pH-control during the experiment. The surplus of medium was pumped away via a metal sampling tube fixed at a certain level fixing the liquid height and volume (1.64 L) inside the bioreactor. Stirring and gassing were maintained at 300 rpm and  $200 \text{ mLn h}^{-1}$ , respectively. Biocalorimeter power was monitored for 2 days in a row just like several temperatures, and off-gas composition.

After monitoring the 'power baseline' the pH was increased to 6.7 adding from the  $NH_4OH$  solution. Afterwards the BioRC1 was inoculated with 20 mL of algal culture grown under mild fluorescent light as described before. Surplus medium was pumped away in order to remain with a constant liquid volume and height. Lamps were turned on and growth was monitored on-line as calorimeter power, gas exchange and pH-control-mediated ammonium hydroxide addition. Off-line samples were used to measure the increase in cell number and volume and ammonium concentration, as described below.

The experiments were ended in the 'linear' phase of growth. Inhibitors of photosynthetic electron transport were added and, subsequently, the gas mixture (oxygen/carbon dioxide/nitrogen, 18/2/80%, v/v/v) was replaced with pure nitrogen of equal flow rate. The system was allowed to equilibrate at a higher power and pH. Finally, the lamps were turned off and the system was allowed to equilibrate and left like this for another 2 days to monitor the power 'baseline'.

During the complete experiment, baseline monitoring, growth monitoring, followed by baseline monitoring, the heat transfer coefficient of the BioRC1 was calibrated every 2nd day. The power was recalculated afterwards using the heat transfer coefficient measured in that specific period of the experiment. Furthermore, during growth ammonium hydroxide solution was pumped into the reactor at a rate determined by the pH-control. In order to remain with a constant liquid volume and height, surplus liquid was pumped out every 2nd hour via the sample tube fixed at the appropriate height.

## 2.4. Chemicals and analyses

### 2.4.1. Inhibitors

Photosynthesis was stopped with two different inhibitors, DCMU (3-(3,4-dichlorophenyl)-1,1-dimethylurea) was used at 40  $\mu\text{M}$  to stop linear electron transport at photosystem II and DBMIB (2,5-dibromo-3-methyl-6-isopropyl-*p*-benzoquinone) was used at 4  $\mu\text{M}$  to inhibit cyclic electron transport around photosystem I. DCMU was injected dissolved in 1.0 mL ethanol and DBMIB dissolved in 1.0 mL chloroform.

### 2.4.2. Sampling

The lower point of the sampling tube was fixed at the liquid level required. The sampling pump was turned on every 2 h for 5 min. In this way a sample was collected of the same volume as the amount of ammonium hydroxide ( $\text{NH}_4\text{OH}$ ) solution added during that 2-h period, hence higher growth led to larger samples. Each 2-hourly sample was collected in a separate glass tube and cooled to +1  $^\circ\text{C}$ . The samples were left like this for 0–16 h before analysis.

### 2.4.3. Data acquisition

The power of the calorimeter was continuously monitored, just like the temperature of the reactor liquid ( $T_r$ ) and the temperature of the oil entering the cooling jacket ( $T_j$ ). The ambient temperature ( $T_{\text{amb}}$ ) was monitored using a PT1000 probe. Also the ambient temperature between the reactor jacket and polycarbonate cylinder ( $T_{\text{amb},j}$ , Fig. 1), and the temperature of the head plate ( $T_{\text{hp}}$ ), were measured continuously using PT1000s. These parameters were logged via a Field-Point data acquisition module and a PCI card of National Instruments (Austin TX, USA). Using LabView software from National Instruments the data acquisition was programmed such that every second all data were collected. One-minute average values were stored each minute in a data file. Off-gas composition, pH, DO, light intensity and the weight of  $\text{NH}_4\text{OH}$  solution added were connected to the same data acquisition system.

### 2.4.4. Cell number and cell volume

Cell number and cell volume were measured with a Coulter Counter ZM and a Channelyzer 256 (Beckman Coulter, Fullerton CA, USA). A 70  $\mu\text{m}$  diameter sample tube was used and the Multisizer was calibrated using 10  $\mu\text{m}$  Latex particles (Beckman Coulter). The instrument settings were: current, 500 mA; attenuation 4; gain, 2. Samples were diluted with an isotonic salt

solution 'Isoton' (Beckman Coulter) to reach a cell concentration between  $1 \times 10^5$  and  $2 \times 10^5$  cells  $\text{mL}^{-1}$  in the samples to be counted.

### 2.4.5. Ammonium

Raw samples (1.5 mL) for ammonium analysis were first centrifuged in an Eppendorf tube (14,000 rpm, 10 min). The supernatant was filtered (0.2  $\mu\text{m}$ ), collected and stored at  $-18^\circ\text{C}$  until analysis. Ammonium in these samples was determined by an enzymatic bioassay of Roche (E1112732, distributed by R-Biopharm AG, Darmstadt, Germany) on a Cobas Mira chemistry system (Roche, Basel, Switzerland).

### 2.4.6. Off-gas analysis

BioRC1 off-gas was analyzed for the volume fraction oxygen ( $\text{O}_2$ ) and carbon dioxide ( $\text{CO}_2$ ). The gas flow from the BioRC1 was split in two and led over two analyzers. The oxygen fraction was measured with a Servomex (Crowborough, England) series 1100 paramagnetic analyzer. Carbon dioxide was determined with a Servomex Xendos 2500 infrared analyzer. During the experiment the gas analyzers were calibrated daily using certified gas mixtures of oxygen and carbon dioxide in nitrogen gas.

## 3. Results and discussion

### 3.1. Modeling power baseline under varying ambient temperature

The BioRC1 calorimeter used is a high sensitivity calorimeter. In previous experiments (data not shown) it was found that baseline stability is affected by variations in ambient temperature. Considering the fact that the heat exchange rate for phototrophic processes is low, baseline stability was monitored and the influence of changing ambient temperature on biocalorimeter power was modeled.

Three possible routes of heat losses (or gains) were identified: (1) reactor inserts extending into the culture broth make up a heat bridge between reactor liquid at  $T_r$  and ambient air at  $T_{\text{amb}}$ . (2) The reactor head plate was maintained at constant temperature,  $T_{\text{hp}}$ , which was 2  $^\circ\text{C}$  higher than  $T_r$ . But, temperature control was not perfect and  $T_{\text{hp}}$  varied with changing ambient temperature and this could lead to variations in biocalorimeter power. (3) The temperature of the oil circulating through the cooling jacket,  $T_j$ , is assumed to be constant and equal to the temperature of the ingoing oil actually measured. It has been shown that temperature gradients exist over the BioRC1 oil jacket [15] as a result of heat exchange with the reactor contents and, possibly, as a result of heat exchange with the ambient air. The average temperature of the oil jacket, and hence biocalorimeter power, therefore could have been influenced by the temperature of the air adjacent to the jacket,  $T_{\text{amb},j}$  (Fig. 1).

The heat flows resulting from the first two heat transfer routes were assumed to be linearly correlated to the corresponding temperature gradients by means of a heat transfer coefficient

(UA).

$$q_{r \rightarrow \text{amb}} = UA_{r \rightarrow \text{amb}} \cdot (T_r - T_{\text{amb}}) \quad (2)$$

$$q_{r \rightarrow \text{hp}} = UA_{r \rightarrow \text{hp}} \cdot (T_r - T_{\text{hp}}) \quad (3)$$

At a  $T_r$  of 37 °C the first process (Eq. (2)) leads to a heat flow directed from the reactor liquid towards the ambient air. The second process (Eq. (3)) leads to a heat flow towards the reactor contents since the head plate is maintained at a higher temperature than the reactor liquid. The third process as such does not describe a leaky heat flow into, or, out of, the reactor liquid and was also not included in our modeling approach. This heat flow, however, could lead to changes in the average temperature of the oil in the jacket. Considering the magnitude of UA (Eq. (1)), 6.65 mW mK<sup>-1</sup>, a change of  $T_j$  of a few mK could already lead to a significant change of biocalorimeter power. Because  $T_j$  is assumed to be equal to the temperature of the incoming oil measured (Fig. 1), variations in the real  $T_j$  cannot be recognized. This disturbance could be accounted for practically by recalibrating the UA and this was done every 2 days in our experiments. Within these 2 days, however, such an effect could have caused residual variation in biocalorimeter power for which we were not able to correct.

In order to correct for baseline variations the first 2 days of each experiment were used to monitor changes in ambient temperature and power baseline. After the cultivation this was repeated for another 2 days as explained in the materials and methods. First, the changes in temperature gradients and biocalorimeter power were normalized with respect to an arbitrary reference period. For batch cultivation 1 (Fig. 2) this reference period was chosen between 29 and 30 h. The actual cultivation was started after 57 h when the reactor was inoculated and the lamps were turned on. The cultivation was ended after 182 h when cellular metabolism was inhibited and the lamps were turned off. The cultivation period between 57 and 182 h is not shown in Fig. 2.

As can be seen in Fig. 2, temperature fluctuations in the laboratory were considerable. During batch 1 the temperature in the laboratory ( $T_{\text{amb}}$ ) increased over 4 °C within a week due to a heat wave outside. This can be seen by the change in  $(T_r - T_{\text{amb}})$ , represented as  $\Delta(T_r - T_{\text{amb}})$ :  $T_r$  is maintained at 37 °C so that a  $\Delta(T_r - T_{\text{amb}})$  of -4 °C implies an increase in  $T_{\text{amb}}$  of 4 °C. Also fluctuations of 2 °C were common within the 24-h day/24-h night cycle, especially when the sun rays hit the laboratories' east-facing windows in the morning  $T_{\text{amb}}$  increased quickly. Temperature of the head plate was much more stable because it was controlled by means of circulating water from a water bath. But, changes in ambient temperature also influenced the head plate temperature ( $T_{\text{hp}}$ ) which increased with almost 0.1 °C during the course of the experiment.

Although it was not used in our baseline model, the temperature gradient between the oil jacket of the BioRC1 ( $T_j$ ) and the air within the confined space between reactor wall and polycarbonate cylinder ( $T_{\text{amb},j}$ , Fig. 1) was also measured. It can be seen that the change of this temperature gradient was less than the one between reactor and the 'free' air in the laboratory. This proves that heat exchange exists between the oil jacket and the

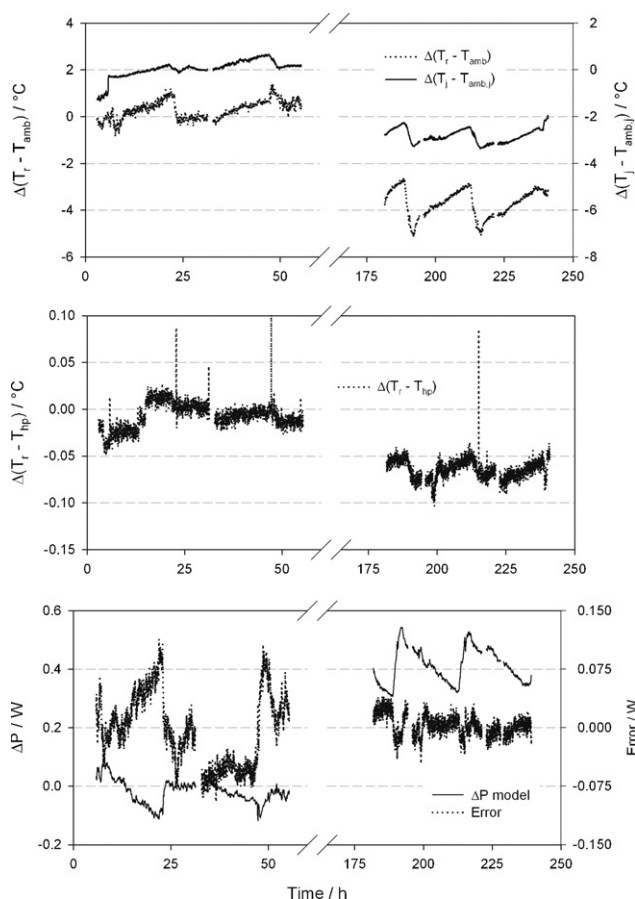


Fig. 2. Modeling of the variation in BioRC1 power ( $P$ ) as a result of variations in ambient temperature before and after batch cultivation 1. Abbreviations:  $T_r$ ,  $T_j$ ,  $T_{\text{amb}}$ ,  $T_{\text{amb},j}$ ,  $T_{\text{hp}}$ , see Fig. 1;  $P$ , calorimeter power. The 'Δ' sign represents the change in the corresponding gradient as referred to the average gradient between 29 and 30 h, the reference period. Fitted heat transfer coefficients:  $UA_{r \rightarrow \text{amb}} = -0.08252 \text{ W } ^\circ\text{C}^{-1}$  and  $UA_{r \rightarrow \text{hp}} = -1.639 \text{ W } ^\circ\text{C}^{-1}$ . With an expected value of '0' the standard deviation of the error is 33 mW.

surrounding air. The influence of this effect on biocalorimeter power measured could be removed by measuring the temperature of the outgoing oil too. In this way ' $T_{j,\text{in}}$ ' and ' $T_{j,\text{out}}$ ' could be averaged to obtain a real  $T_j$  which can be entered in Eq. (1). For this the BioRC1 measurement and control circuitry needs to be adapted by the manufacturer.

The variation in the power baseline of the BioRC1 recorded 2 days before and after the cultivation was modeled according to Eq. (4). The heat transfer coefficients  $UA_{r \rightarrow \text{amb}}$  and  $UA_{r \rightarrow \text{hp}}$  were estimated by an iterative procedure minimizing the sum of the error squared (Eq. (5)).

$$\Delta P_{\text{model}} = UA_{r \rightarrow \text{amb}} \cdot \Delta(T_r - T_{\text{amb}}) + UA_{r \rightarrow \text{hp}} \cdot \Delta(T_r - T_{\text{hp}})$$

$$\text{and : } \Delta(T_r - T_{\text{amb}}) = (T_r - T_{\text{amb}}) - (T_r - T_{\text{amb}})_{\text{reference}}, \text{ etc.} \quad (4)$$

$$\text{Error} = \Delta P - \Delta P_{\text{model}} \quad (5)$$

$$\text{and : } \Delta P = P - P_{\text{reference}}$$

The result of this model,  $\Delta P_{\text{model}}$ , is shown in lower graph of Fig. 2 and it is compared to the error still present. Especially when the ambient temperature in the laboratory changes quickly

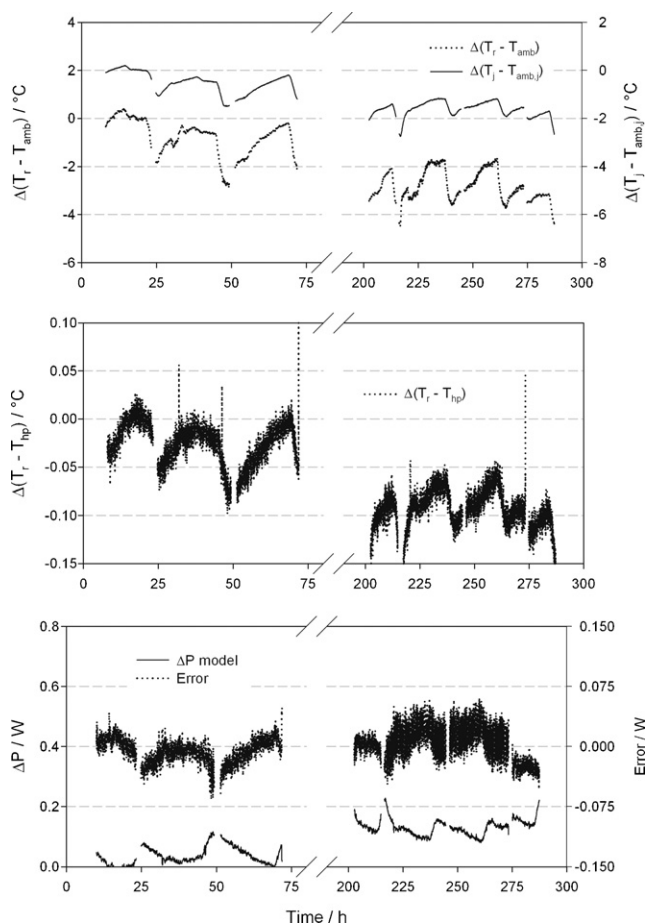


Fig. 3. Modeling of the variation in BioRC1 power ( $P$ ) as a result of variations in ambient temperature during batch cultivation 2. See Fig. 2 for more details. Fitted heat transfer coefficients:  $UA_{r \rightarrow \text{amb}} = -0.00180 \text{ W } ^\circ\text{C}^{-1}$  and  $UA_{r \rightarrow \text{hp}} = -1.350 \text{ W } ^\circ\text{C}^{-1}$ . With an expected value of '0' the standard deviation of the error is 17 mW.

(in the morning) there is still residual variance within the baseline for which cannot be corrected. The standard deviation of the error during whole the period of baseline monitoring was 33 mW with the accuracy increasing towards the end of the experiment.

During batch 2 it was attempted to insulate the head plate. A hollow cylinder of 20 cm height was placed on top of the table supporting the bioreactor. This cylinder enclosed the head plate and the larger part of the inserts extending above the head plate and it was completely filled with cotton wool. As can be seen in Fig. 3 the residual error was reduced. The standard deviation of the error, which should be zero, was 17 mW. The effect of head plate insulation was also visible in the heat transfer coefficients fitted,  $UA_{r \rightarrow \text{amb}}$  and  $UA_{r \rightarrow \text{hp}}$ . These were smaller during batch cultivation 2 (numerical values in legends Figs. 2 and 3).

### 3.2. Heat exchange during photoautotrophic batch growth

The goal of this study was to monitor batch growth of photoautotrophic microalgae quantitatively by calorimetry. In Fig. 4 the growth of *C. sorokiniana* in the BioRC1 is presented. After 57 h the reactor was inoculated with 20 mL of algal suspension and the lamps were turned on. Within 20 h from inoculation

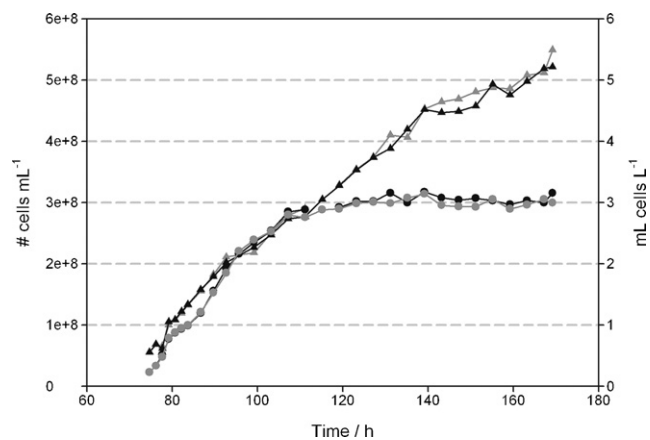


Fig. 4. Growth of *Chlorella sorokiniana* during batch cultivation 1. Circles (●) represent biomass concentration as number of cells per millilitre culture broth and triangles (▲) represent millilitre biovolume per litre culture broth as determined using the Coulter Counter. Ash-free cell dry weight varied between 500 and 550 mg mL<sup>-1</sup> biovolume.

growth is clearly visible as an increase in cell number and biovolume. An exponential growth phase is difficult to distinguish, possibly during the first 30 h after inoculation. After this period, microalgal growth can be described with a linear biomass increase although the rate of increase starts to deviate quickly from linearity and decreases. Such a pro-longed (linear) growth after a short exponential growth phase is characteristic for photoautotrophic growth, the rate of which is determined by the constant supply of light energy [17]. An interesting observation is that after 120 h the cell number does not increase anymore. Cell size still increases resulting in a steady increase in biovolume. As will be shown later, growth was inhibited after 169 h and at this point the biovolume had increased to more than 5 mL L<sup>-1</sup> corresponding to more than 2.5 g dry weight L<sup>-1</sup>.

The measurement of biovolume was used to calculate the rate of biomass increase at each sample point during the cultivation. This rate clearly shows a quick rise up to the point around 80 h when the maximal biomass productivity is reached (Fig. 5). As time progressed the production rate slowly decreased up to the point the cultivation was stopped. In the same fig-

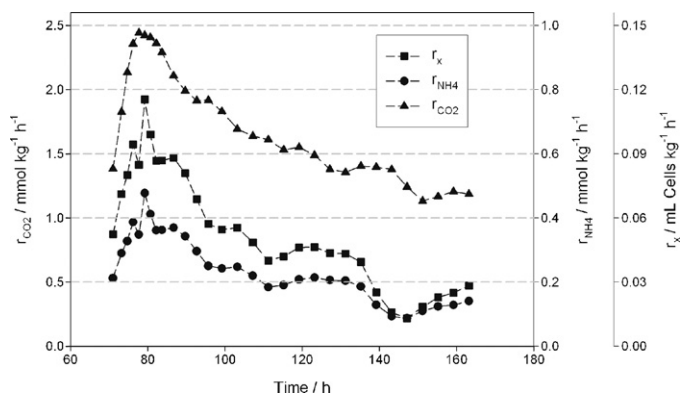


Fig. 5. Carbon dioxide consumption rate (▲,  $r_{\text{CO}_2}$ ), ammonium consumption rate (●,  $r_{\text{NH}_4}$ ) and biomass production rate (■,  $r_x$ ) during batch cultivation 1. All rates are defined as positive values and expressed per kilogram of culture broth.

ure the carbon dioxide and ammonium consumption rates are plotted. They show the same trend: a fast rise to the maximum consumption rate reached after 80 h followed by a slow but continuous decrease as the cultivation progressed. The maximum rates reached after 80 h most likely reflect the fact that at this point the biomass density was such that all the light energy entering the reactor was absorbed within the culture broth and no light could escape anymore.

The complete and corrected BioRC1 power trace ( $P_{\text{corrected}}$ ) recorded during batch cultivation 1 is shown in Fig. 6. The heat transfer coefficient  $UA$  was determined every 2nd day using a calibration heater and this can be seen in Fig. 6 as the regularly occurring peaks. The raw power ( $P$ ), derived from  $T_r$  and  $T_j$  (Eq. (1)), was corrected for baseline variations using Eq. (6) to obtain  $P_{\text{corrected}}$ . The calculation of  $\Delta P_{\text{model}}$  and the parameters herein have been explained in the previous section.

$$P_{\text{corrected}} = P - \Delta P_{\text{model}} \text{ and therefore :} \quad (6)$$

$$P_{\text{corrected}} = P - UA_{r \rightarrow \text{amb}} \cdot \Delta(T_r - T_{\text{amb}}) - UA_{r \rightarrow \text{hp}} \cdot \Delta(T_r - T_{\text{hp}})$$

After inoculating the reactor and turning on the illumination, biocalorimeter power increased sharply (Fig. 6). This is related to the fact that a considerable part of the light energy is absorbed within the reactor by the microalgae and by the reactor inserts (pH and DO sensors, stirrer and sparger). The baffles were removed from the BioRC1 to prevent light absorption by these inserts. The major part of the light energy absorbed will be dissipated as heat and hence will lead to the sharp increase in power observed. After this initial step-wise increase, the power increases more smoothly. The multiplying cells intercept an increasing fraction of the light and, as will be shown later, after

80 h no light entering the BioRC1 could escape anymore: all light was absorbed by the microalgae.

The insert of Fig. 6 shows the changes in calorimeter power at the end of the cultivation in more detail. After 169 h inhibitors of photosynthetic electron transport were added: DCMU and DBIMB. This led to an unexpected and quick induction of respiratory activity resulting in a significant increase in biocalorimeter power. Turning off the light the respiratory activity slowly decreased (data not shown). The power, on the other hand, dropped dramatically ( $t = 173$  h, in Fig. 6), but this was directly related to the removal of light-induced heat dissipation within the culture. Turning the lamps on again, a few hours later, the respiratory activity returned to the old elevated level. There was only one way to stop all metabolic activity and that was replacing the gas mixture composed of oxygen, carbon dioxide and nitrogen with pure nitrogen. As can be seen in the insert of Fig. 6, this resulted in a constant power at time equals 180 h representing the dissipation of all light energy as heat inside the culture broth, and this level is referred to as  $P_{\text{max}}$ .

The dynamic effects observed during the forced ending of photoautotrophic metabolism will be discussed in more detail in the next section. First, the translation of the measured calorimeter power into biochemical activity will be presented. The difference between the power ( $P_{\text{corrected}}$ ) during photoautotrophic growth and the power after inhibiting metabolism,  $P_{\text{max}}$ , gives the biochemical heat flow,  $q_{\text{bio}}$ . The variable  $q_{\text{bio}}$  is presented in Figs. 7 and 9, and its calculation from these power levels is shown in Eq. (7). It has a positive value since photosynthesis is considered to be an endothermic process because it consumes and stores light energy which otherwise would have been dissipated as heat.

$$q_{\text{bio}} = P_{\text{max}} - P_{\text{corrected}} \quad (7)$$

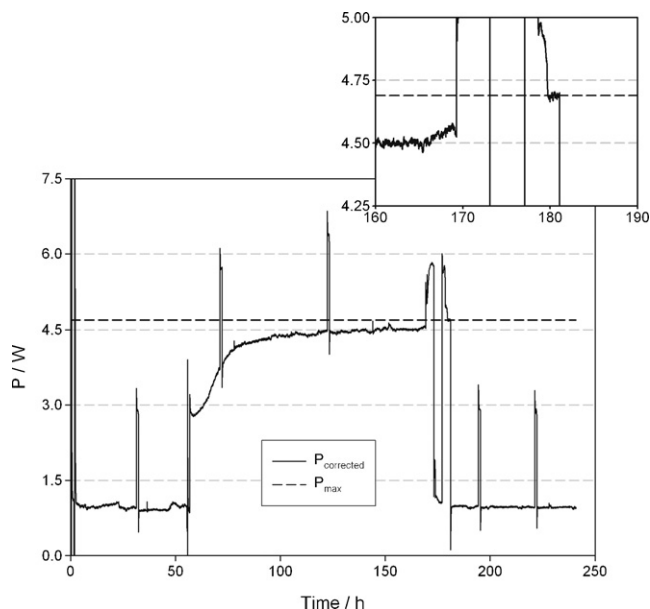


Fig. 6. Biocalorimeter power during batch cultivation 1 of *Chlorella sorokiniana* in the BioRC1 calorimeter. The parameter  $P_{\text{corrected}}$  represents the calorimeter power corrected for the fluctuations of ambient temperature. After 57 h the reactor was inoculated and lamps were turned on. The inserts shows more detail of the end of the experiment when metabolism was stopped to measure the power with all light absorbed being converted to heat. This maximal power,  $P_{\text{max}}$ , is represented by the dashed line.

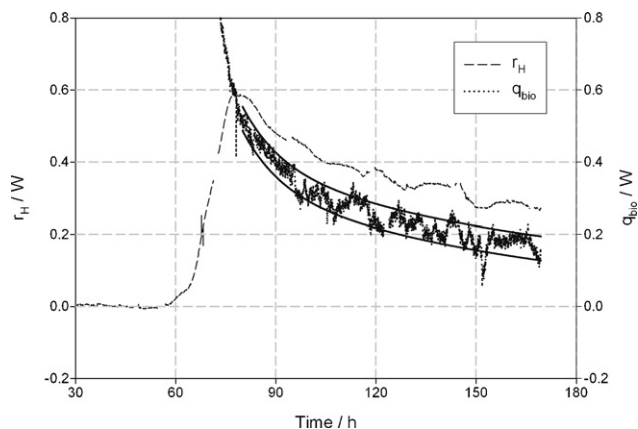


Fig. 7. Measured and calculated heat exchange rate during photoautotrophic culture of *Chlorella sorokiniana* in the BioRC1; batch cultivation 1. Light input measured was 3.72 W. After 57 h the reactor was inoculated and the lamps were turned on. The dashed line ( $r_H$ ) gives the enthalpy production rate calculated from the rate of biochemical reactions in the BioRC1 (Eq. (8)). The dotted line gives the heat exchange rate measured ( $q_{\text{bio}}$ ). The two solid lines give the range covered by the average  $q_{\text{bio}}$  plus/minus the standard deviation as determined during baseline modeling. The standard deviation of the error remaining after baseline modeling was 33 mW (Fig. 2). The average was fitted using a 5-parameter double exponential decay model describing the decreasing trend from 80 h onwards well (adjusted  $r^2 = 0.93$ ).

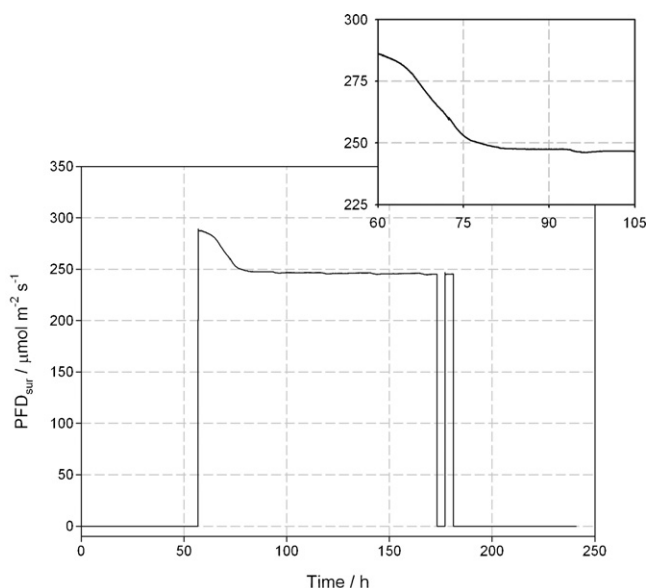


Fig. 8. Photon flux density at reactor surface ( $PFD_{sur}$ ) as measured with spherical light sensor during batch cultivation 1 (see Fig. 1 for sensor position). After 57 h the reactor was inoculated and lamps were turned on. The inserts shows more detail on the period in which the biomass in the reactor reached such a density that no light was passing through anymore.

The variable  $q_{bio}$  plotted corresponds to the real biochemical activity only if all light entering the bioreactor is absorbed. At very low biomass density a considerable part of the light energy can escape the bioreactor again. This explains the unrealistically high  $q_{bio}$  observed before time equals 80 h (Fig. 7). The measurement of the photon flux density at the reactor surface illustrates this. Although the spherical sensor ‘faces’ the light source (the reactor side was shielded) it was observed that the light intensity during the first 30 h after inoculation is higher (Fig. 8). This must have been caused by light escaping the bioreactor and falling on the sensor via reflections on the structures surrounding the bioreactor (Fig. 1) This effect provided a means to determine when

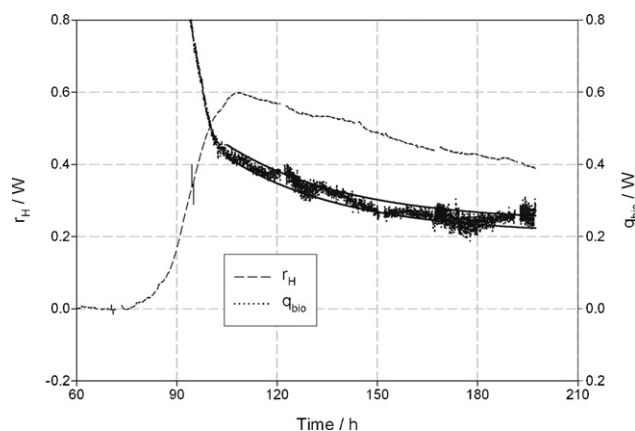


Fig. 9. Measured ( $q_{bio}$ ) and calculated ( $r_H$ ) heat exchange rate during photoautotrophic culture of *Chlorella sorokiniana* in the BioRC1; batch cultivation 2. Light input was 3.46 W. See Fig. 7 for more details. After 73.5 h the reactor was inoculated and the lamps were turned on. The standard deviation of the error remaining after baseline modeling was 17 mW (Fig. 3). The adjusted  $r^2$  after fitting the average  $q_{bio}$  using a double exponential decay model was 0.92.

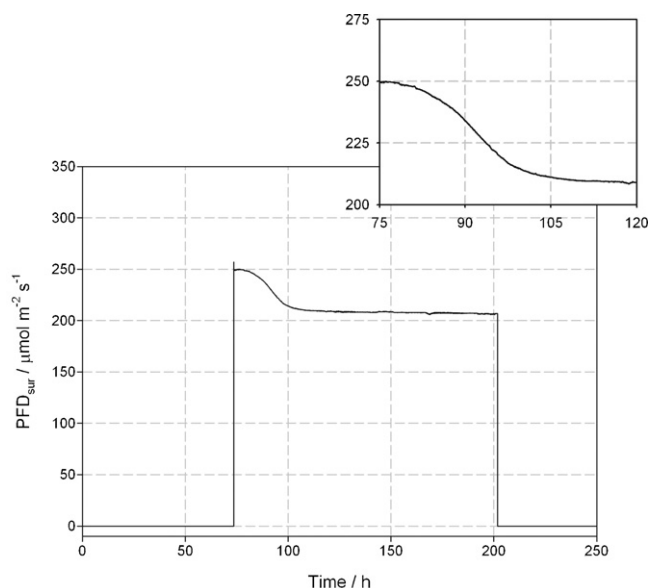


Fig. 10. Photon flux density ( $PFD_{sur}$ ) at reactor surface as measured with spherical light sensor during batch cultivation 2. After 73.5 h the reactor was inoculated and lamps were turned on. See Fig. 8 for more details.

all light was absorbed within the reactor and when the variable  $q_{bio}$  reflects solely biochemical activity: at time equals 80 h for batch cultivation 1 and time equals 105 h for batch 2 (Fig. 10).

The other variable plotted in Figs. 7 and 9,  $r_H$ , represents the biochemical enthalpy production rate within the BioRC1 calculated from the consumption rates of carbon dioxide and ammonium hydroxide. The biochemical reactions within the reactor are illustrated in Fig. 11. The enthalpy change is determined by the rate of biomass growth and to a low extent (less than 3% of  $r_H$ ) by the rate of the neutralization reaction. The rate of neutralization is equal to the molar rate of ammonium hydroxide consumption ( $r_{NH_4}$ ), but of opposite sign. The molar rate of biomass increase is equal to the molar rate of carbon

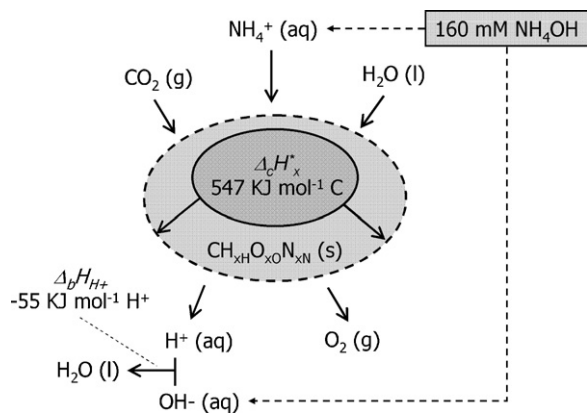


Fig. 11. Schematic representation of the biochemical reactions during photoautotrophic growth and associated enthalpy changes. All substrates and products can be considered to be in their reference states with exception of the product biomass,  $CH_xH_yO_xO_N_xN(s)$ . The modified enthalpy of combustion,  $\Delta_cH_x^*$ , of *Chlorella* biomass was taken from Duboc et al. [18].  $\Delta_bH_{H^+}$  is the enthalpy of neutralization of protons ( $H^+$ ). Ammonium and hydroxide ions were added as a diluted  $NH_4OH$  solution. Carbon dioxide ( $CO_2$ ) was added via the gas phase. Oxygen ( $O_2$ ) was removed via the gas phase.



dioxide consumption ( $r_{\text{CO}_2}$ ), but of opposite sign. The enthalpy of combustion of biomass is equal to the energy stored per unit of biomass, but again of opposite sign. As such,  $r_{\text{H}}$  can be calculated according to Eq. (8). This calculation results in a positive value for the enthalpy production rate reflecting the endothermic nature of photosynthesis, a process which stores light energy that would have been dissipated as heat otherwise (Figs. 7 and 9).

$$r_{\text{H}} = r_{\text{CO}_2} \cdot \Delta_c H_x^* + r_{\text{NH}_4} \cdot -1 \cdot \Delta_b H_{\text{H}^+} \quad (\text{see also Fig. 11}) \quad (8)$$

$r_{\text{CO}_2}$  and  $r_{\text{NH}_4}$  are negative quantities since they represent consumption.

The variable  $q_{\text{bio}}$  can only be used after time equals 80 h, as explained above. In Fig. 7 it can be seen that  $q_{\text{bio}}$  decreases from 0.52 W at 80 h to 0.20 W at the end of the experiment. Taking into consideration the light input measured (3.72 W as explained later) this corresponds to a photosynthetic efficiency of 14% at 80 h decreasing to 5.4% at the end of the experiment. The photosynthetic efficiency gives the fraction of light energy which is stored as chemical energy (i.e. biomass).

Taking  $r_{\text{H}}$  we see that the maximal enthalpy production rate is almost 0.60 W, which would correspond to a photosynthetic efficiency of 16%. After this maximum also  $r_{\text{H}}$  decreases, in a similar fashion as  $q_{\text{bio}}$ , to a value of 0.28 W (Fig. 7). It should be noted that the photosynthetic efficiency calculated was not corrected yet for the exothermic effect of the neutralization reaction (Fig. 11) which is both present in the variables  $q_{\text{bio}}$  and  $r_{\text{H}}$ . But, this reaction has a marginal influence and was therefore neglected.

Because the cultivations were performed under constant pressure the heat flow measured using calorimetry,  $q_{\text{bio}}$ , should be equal to the enthalpy production rate calculated using Eq. (8),  $r_{\text{H}}$ . However,  $q_{\text{bio}}$  is always lower than  $r_{\text{H}}$ . There seems to be an offset in one, or both, of the measurements. It could be related to the measurement of  $q_{\text{bio}}$ , more specifically  $P_{\text{max}}$ , which will be discussed later.

The enthalpy of combustion used was taken from another *Chlorella* strain and will be different from the enthalpy of combustion of our strain. Considering that values for the enthalpy of combustion do not vary more than maximally  $\pm 10\%$  [18], such an error cannot fully explain the offset observed between  $q_{\text{bio}}$  and  $r_{\text{H}}$ . In addition, the calculation of  $r_{\text{H}}$  is based on constant biomass composition with constant enthalpy of combustion. Probably these characteristics will change during the course of the experiment leading to a discrepancy between  $r_{\text{H}}$  and  $q_{\text{bio}}$ . With no other disturbing factors present, the combination of calorimetry and on-line measurement of carbon dioxide exchange could in fact visualize such changes during a cultivation.

Despite the fact that  $q_{\text{bio}}$  does not exactly match  $r_{\text{H}}$ , the variable  $q_{\text{bio}}$  gives a meaningful representation of photoautotrophic growth. These results clearly show that biocalorimetry can be used to monitor microalgal growth on-line and can provide additional information. The results of batch cultivation 2 show the same trend (Fig. 9). The photosynthetic activity is highest in the first phase of batch growth and then slowly decreases up to the time the cultivation was stopped. Based on the variable  $q_{\text{bio}}$

photoautotrophic storage of light energy was 0.44 W on time equals 105 h and decreased to 0.26 W just before the cultivation was stopped. The maximum activity found as based on  $r_{\text{H}}$  was exactly equal to the one found during the first cultivation, 0.6 W.

During the second batch cell growth appeared to have reduced at a lower rate after reaching the maximum rate in the beginning of the experiment. Within the same period of time after reaching the maximal activity (90 h) more biomass appeared to have been produced during batch cultivation 2. At the end of the second experiment a cell density of 7 mL cells  $\text{L}^{-1}$  of culture broth was reached. The explanation behind this different behavior is still lacking, but it could be clearly demonstrated with both the on-line measurement of  $q_{\text{bio}}$  and  $r_{\text{H}}$  and it was also confirmed by the rate of consumption of ammonium (data not shown) illustrating the potential of these techniques.

The performance of the LED-based light source used was satisfactory. A constant output was a prerequisite to be able to measure the biochemical heat flow,  $q_{\text{bio}}$ . The light intensity measured with the photon flux density sensor at the reactor wall was constant after the initial decrease discussed before (Figs. 8 and 10). This proves that the LED output did not decrease significantly. Taking a very detailed look, however, a small decrease of the photon flux could be observed (1–1.5%). This decrease was linearly correlated with the increase in room temperature. This was proven by the fact that also the daily day–night-induced temperature fluctuations had a similar effect on the photon flux density measured. The temperature change could have influenced the actual measurement but it is more likely that the temperature increase directly reduced LED output. In the latter case such an effect could partly explain the discrepancy between  $q_{\text{bio}}$  and  $r_{\text{H}}$ . Technically also this issue could be resolved minimizing fluctuations in ambient temperature.

### 3.3. Biocalorimeter power without biological activity: determination of light input

For the measurement of the biochemical heat flow,  $q_{\text{bio}}$ , it was needed to accurately determine the input of light energy. This was done at the end of the cultivation inhibiting microalgal metabolism without inducing cell death. Cell death and cell lyses had to be prevented because this would lead to changes in light absorption characteristics of the culture broth. To illustrate this procedure the changes of different process variables during inhibition of batch cultivation 2 are presented in Fig. 12.

The first approach was the inhibition of metabolism with inhibitors of the photosynthetic electron transport chain as was done in our previous study [11]. The inhibitors DCMU and DBIMB were added after 198.5 h. The shift from carbon dioxide consumption to carbon dioxide evolution and the shift from oxygen evolution to oxygen consumption clearly show that a respiratory process became active, the rate of which was considerably higher than the rate of photosynthesis before adding the inhibitors. Also the biochemical heat flow measured changed from endothermic to strongly exothermic. The consumption of ammonium hydroxide increased strongly which is related to the accumulation of carbon dioxide in the culture broth. As a result of the hydroxide addition the pH remained constant.

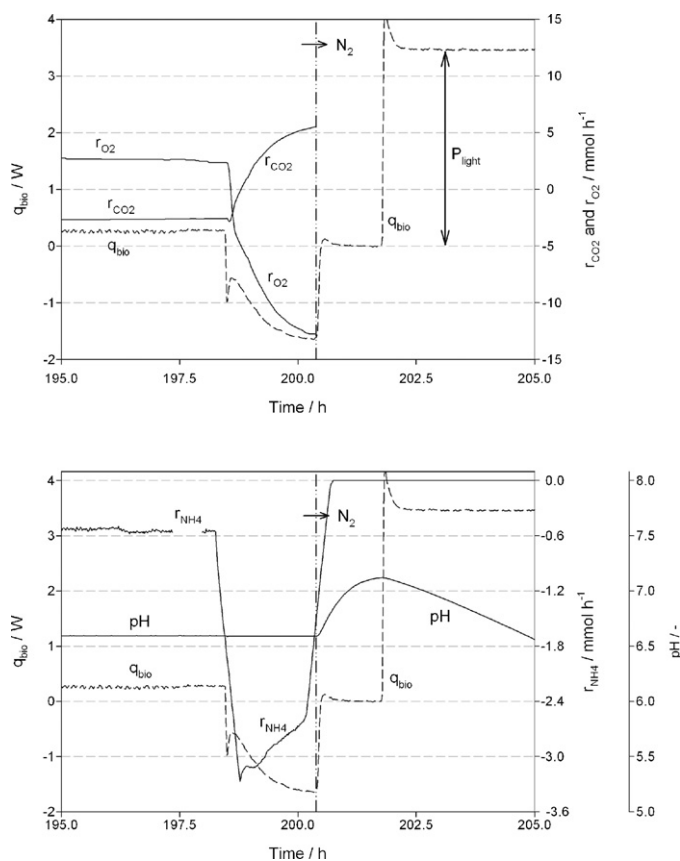


Fig. 12. Changes in biochemical rates and process conditions at the end of batch cultivation 2. At  $t = 198.5$  h inhibitors of photosynthetic electron transport were added. Subsequently, at  $t = 200.4$  h the gas mixture was replaced with pure nitrogen. Finally, at  $t = 201.7$  h the lamps were turned off. In the upper graph the measured heat exchange rate ( $q_{\text{bio}}$ ) and the carbon dioxide and oxygen production rates ( $r_{\text{CO}_2}$  and  $r_{\text{O}_2}$ ) are plotted. In the lower graph  $q_{\text{bio}}$ , the ammonium consumption rate ( $r_{\text{NH}_4}$ ) and the pH are presented. Consumption rates are presented as negative values.

The induction of respiration was not expected because it was not observed at all in our previous study with the microalga *C. vulgaris* [11]. *C. sorokiniana*, apparently behaves completely differently. It is a high temperature strain exhibiting a high maximal specific growth rate ( $0.24 \text{ h}^{-1}$ ) and able to grow as fast under mixotrophic and heterotrophic conditions [19]. This has been verified in our laboratory too (data not shown) and apparently this alga exhibits a high respiratory capacity. It seems therefore that at the end of the cultivation the microalgae accumulated large amounts of easily accessible carbohydrates which were rapidly respired as soon as photosynthetic electron transport was inhibited. During the final stage of cultivation 1 the lamps were turned off for some time before switching to nitrogen gassing. The respiratory activity then slowly decreased to a level 5 times as low (data not shown). As soon as the lamps were turned on again, respiration returned to the old, elevated, level. It appears therefore that the high rate of respiration is induced by the combination of light supply and addition of photosynthetic electron transport inhibitors.

Although these were interesting findings the respiratory activity prevented the determination of the real input of light

energy. This was resolved by replacing the oxygen/carbon dioxide/nitrogen gas mixture with pure nitrogen. In this way essential reactants for both photosynthesis and respiration were purged out of the culture broth and all metabolic activity was stopped. The switch to nitrogen was done after 200.4 h and it can be seen that  $q_{\text{bio}}$  quickly approached '0' (Fig. 12). This is not surprising since the power measured under these circumstances,  $P_{\text{max}}$ , was used as the reference signal to calculate  $q_{\text{bio}}$  (Eq. (7)).

After 201.7 h, the lamps were turned off and  $q_{\text{bio}}$  quickly increased to a new stable value of 3.46 W (Fig. 12). This is equal to the light input into the culture broth during cultivation. The value of  $q_{\text{bio}}$  with the LEDs turned off corresponds to the baseline power as it was used to model the influence of changing ambient temperature as presented and discussed earlier. The BioRC1 was left in this situation for another 2 days maintaining the same rate of stirring and gassing.

There was no additional independent technique to verify whether this procedure to determine the light energy input was correct. The fact that  $q_{\text{bio}}$  determined calorimetrically is consistently lower than the  $r_{\text{H}}$  calculated from the carbon dioxide and ammonium hydroxide consumption rates could indicate that this procedure is not fully correct. But, as discussed before, there are other, partial, explanations for the discrepancy between  $q_{\text{bio}}$  and  $r_{\text{H}}$ .

A possible source of error in the measurement of  $q_{\text{bio}}$  could be the induction of fluorescence as a result of the addition of the photosynthesis inhibitor DCMU. Fluorescence during photoautotrophic growth makes up 0.6–3% of the light energy absorbed [20]. The herbicide DCMU induces a fast fluorescence rise as a result of blocking the re-oxidation of the photosystem II reaction center and, as such, it is often used as a tool to induce maximal fluorescence [21]. Fluorescence therefore could lead to the loss of light energy from the BioRC1 by radiation instead of thermal dissipation in the BioRC1 culture broth. Part of the fluorescence will be absorbed again by other algae within the broth and will still be dissipated as heat. Another part could have escaped from the bioreactor leading to a lower  $P_{\text{max}}$  (Fig. 6) and resulting in an underestimation of  $q_{\text{bio}}$  (Eq. (7)). To check this hypothesis it is necessary to use advanced measurement techniques to detect and quantify fluorescence coming back from the bioreactor.

#### 4. Conclusions

It has been demonstrated that biocalorimetry can be used to study photoautotrophic growth on-line. The application of biocalorimetry in combination with other on-line measurements such as carbon dioxide and oxygen exchange can improve the knowledge on the state of the metabolism. The combined data could, for example, be used to calculate the degree of reduction of the biomass produced at different stages in the bioprocess.

Specifically for photoautotrophic cultures, stringent procedures have to be followed to minimize the influence of external conditions on calorimeter power. Further improvements of the experimental set-up and procedures have been identified and discussed. Most important is the use of a temperature controlled environment. Based on the results shown in Figs. 2 and 3 a tight control within limits of maximally  $\pm 0.5^\circ\text{C}$  is necessary

to improve long-term baseline stability. In such an environment also the performance of electronics such as the LED light source and the BioRC1 measurement and control unit itself will be better with respect to stability. Finally, measurement of the temperature of the outgoing oil of the BioRC1 cooling jacket could further reduce baseline variations and needs to be incorporated by the manufacturer of this calorimeter.

The photosynthetic efficiency is a parameter which is frequently used in the field of microalgal biotechnology [22]. It is an important optimization parameter because light supply usually limits productivity of photobioreactors and hence the photosynthetic efficiency needs to be maximized. The maximal photosynthetic efficiency is a value which is not accurately known. A commonly referred to number is based on a quantum requirement of 12 photons needed to incorporate 1 molecule of carbon (from CO<sub>2</sub>) in algal biomass. Combining this quantum requirement with the energy of a photon of 625 nm and the modified enthalpy of combustion of *Chlorella* [18] (Fig. 11) we find a maximal photosynthetic efficiency of 24%.

The maximal efficiency measured in the BioRC1 was 16%, corresponding to a quantum requirement of 18. Obviously photosynthesis is not running at maximal efficiency. This is easily explained with the fact that the light intensity at the reactor surface is over-saturating. From the calorimetrically determined light input it was calculated that the photon flux density at the reactor surface was 346  $\mu\text{mol m}^{-2} \text{s}^{-1}$  (cultivation 1) and 318  $\mu\text{mol m}^{-2} \text{s}^{-1}$  (cultivation 2). These are saturating intensities, and under these circumstances a considerable part of the photons is not used in photosynthetic electron transport [22]. Their energy is solely dissipated as heat by a combination of mechanisms commonly referred to as non-photochemical quenching [23,24]. Also the demonstration that the photosynthetic efficiency decreases as the biomass density increases fits well with previous findings that an increasing dark zone inside a photobioreactor leads to a decrease in the yield of biomass on light energy [25,26].

The influence of cell density on photosynthetic efficiency led to the development of short light path photobioreactors in which turbulent mixing provided for high photosynthetic efficiencies at high cell densities [27]. The light path of the BioRC1 ( $\varnothing$  11.6 cm) is too long and, as such, it is not representative for state-of-the-art photobioreactors. Applying heat flow calorimetry on bench-scale short light-path photobioreactors is a challenge which

could generate a promising technique to study and optimize photoautotrophic bioprocesses.

## References

- [1] B. Birou, U. von Stockar, *Enzyme Microb. Technol.* 11 (1989) 12–16.
- [2] C. Herwig, I. Marison, U. von Stockar, *Biotechnol. Bioeng.* 75 (2001) 345–354.
- [3] C. Herwig, U. von Stockar, *Bioproc. Biosyst. Eng.* 24 (2002) 395–403.
- [4] P. Duboc, L.G. Cascao-Pereira, U. von Stockar, *Biotechnol. Bioeng.* 57 (1997) 610–619.
- [5] J.L. Magee, T.W. DeWitt, E. Coolidge Smith, F. Daniels, *J. Am. Chem. Soc.* 61 (1939) 3529–3533.
- [6] V.Y. Petrov, A.J. Alyabyev, N.L. Loseva, G.S. Klementyeva, V.I. Tribunskich, *Thermochim. Acta* 251 (1995) 351–356.
- [7] P. Johansson, I. Wadsö, *J. Biochem. Biophys. Methods* 35 (1997) 103–114.
- [8] V.S. Mukhanov, R.B. Kemp, *Thermochim. Acta* 446 (2006) 11–19.
- [9] A.J. Walker, *Trends Plants Sci.* 7 (2002) 183–185.
- [10] R. Patiño, M. Janssen, U. von Stockar, *Biotechnol. Bioeng.* 96 (2006) 757–767.
- [11] M. Janssen, R. Patiño, U. von Stockar, *Thermochim. Acta* 435 (2005) 18–27.
- [12] R.K. Mandalam, B.O. Palsson, *Biotechnol. Bioeng.* 59 (1998) 605–611.
- [13] I. Marison, J.-S. Liu, S. Ampuero, U. von Stockar, B. Schenker, *Thermochim. Acta* 309 (1998) 157–173.
- [14] I. Marison, M. Linder, B. Schenker, *Thermochim. Acta* 310 (1998) 43–46.
- [15] M.C. García-Payo, S. Ampuero, J.-S. Liu, *Thermochim. Acta* 391 (2002) 25–39.
- [16] H.C.P. Matthijs, H. Balke, U.M. Hes van, B.M.A. Kroon, L.R. Mur, R.A. Binot, *Biotechnol. Bioeng.* 50 (1996) 98–107.
- [17] J.C. Ogonna, H. Yada, H. Tanaka, *J. Ferment. Bioeng.* 80 (1995) 259–264.
- [18] P. Duboc, I. Marison, U. von Stockar, in: R.B. Kemp (Ed.), *Handbook of Thermal Analysis and Calorimetry*, Elsevier, 1999, pp. 267–365.
- [19] Y.K. Lee, S.Y. Ding, C.H. Hoe, C.S. Low, *J. Appl. Phycol.* 8 (1996) 163–169.
- [20] G.H. Krause, E. Weis, *Annu. Rev. Plant Physiol. Plant Mol. Biol.* 42 (1991) 313–349.
- [21] S.Z. Tóth, G. Schansker, R.J. Strasser, *Biochim. Biophys. Acta* 1708 (2005) 275–282.
- [22] M. Janssen, J. Tramper, L.R. Mur, R.H. Wijffels, *Biotechnol. Bioeng.* 81 (2003) 193–210.
- [23] P. Müller, X.P. Li, K.K. Niyogi, *Plant Physiol.* 125 (2001) 1558–1566.
- [24] J.A. Cruz, T.J. Avenson, A. Kanazawa, K. Takizawa, G.E. Edwards, D.M. Kramer, *J. Exp. Bot.* 56 (2005) 395–406.
- [25] M. Janssen, M. de Winter, J. Tramper, L.R. Mur, J.F.H. Snel, R.H. Wijffels, *J. Biotechnol.* 78 (2000) 123–137.
- [26] M.J. Barbosa, M. Janssen, N. Ham, J. Tramper, R.H. Wijffels, *Biotechnol. Bioeng.* 82 (2003) 170–179.
- [27] A. Richmond, in: A. Richmond (Ed.), *Handbook of Microalgal Culture*, Blackwell Publishing, 2003, pp. 125–177.